10.1109/ULTSYM.2014.0066

Estimation of Depletion or Injection Induced Changes in Reservoir Stresses using Time-lapse Sonic Data

Bikash K. Sinha
Mathematics and Modeling Department
Schlumberger-Doll Research
Cambridge, Massachusetts, USA
sinha1@slb.com

Ergun Simsek
Department of Electrical and Computer Engineering
The George Washington University
Washington, DC, USA
ergunsimsek@gmail.com

Abstract— **A new technique uses time-lapse borehole sonic data acquired in a vertical borehole parallel to the X_3-axis to estimate changes in formation stresses caused by reservoir depletion or injection. A pre-production baseline survey acquires sonic data in an open or cased hole along with estimates of reservoir pressure, overburden and minimum horizontal stresses. After years of depletion or injection, a monitor survey acquires sonic data in an observation well. Both sonic datasets are processed to obtain the borehole Stoneley and cross-dipole dispersions. An inversion algorithm inverts the measured Stoneley dispersion to estimate the far-field shear modulus C_{66} in the borehole cross-sectional plane. The shear moduli C_{44} and C_{55} in the two orthogonal borehole axial planes are obtained directly from the low-frequency asymptotes of the two cross-line flexural dispersions. Differences in the three shear moduli from the baseline survey yield the maximum horizontal stress magnitude and an acoustoelastic coefficient using the estimated pore pressure, overburden and minimum horizontal stresses. The three far-field shear moduli in the three orthogonal planes are also obtained from the subsequent monitor survey. This algorithm uses the acoustoelastic coefficient from the baseline survey and the three shear moduli after depletion or injection to estimate changes in the maximum and minimum horizontal stress magnitudes caused by reservoir pressure changes.**

Keywords—reservoir stresses, depleted reservoirs, time-lapse sonic

I. INTRODUCTION

Reservoir depletion and subsequent fluid (water and carbon dioxide) injection for enhanced oil recovery cause changes in the reservoir pressure and formation stresses. Large stress changes can cause cap rock fractures and activate pre-existing faults, leading to CO_2 leakage.

Time-lapse seismic can detect acoustic impedance changes on the order of 3 to 9% and they provide qualitative indicators of reservoir pressure and saturation changes. Time-lapse sonic with higher velocity resolution can provide estimates of depletion or injection induced changes in reservoir stresses.

Figure 1 shows a schematic diagram of CO_2 and water injection to enhance hydrocarbon production in a tertiary recovery project. Reservoir depletion or fluid injection for enhanced recovery can lead to two types of structural failure. First, if the reservoir stresses together with pore pressure cause the breakdown pressure P_B in the wellbore to exceed a threshold, cap rock fractures are initiated and reservoir integrity is damaged. To reduce risk of cap rock fractures, the breakdown pressure should be less than the threshold given by the following equation

$$P_B \le 3S_h - S_H - \alpha P_P + T_S \quad , \tag{1}$$

where S_h and S_H are the minimum and maximum horizontal stresses, α is the Biot parameter, P_P is the reservoir pressure, and TS is the rock tensile strength.

Second, if the reservoir pressure P_P exceeds a threshold given by the Coulomb criterion for the initiation of slip along a pre-existing fault, a reactivation of such faults would also cause reservoir damage. To mitigate risk of such slippage, the reservoir pressure must be maintained below a threshold given by

$$P_P \le \sigma_n - \tau/\mu_f + C/\mu_f \quad , \tag{2}$$

$$\sigma_n = S_H \cos^2\theta + S_V \sin^2\theta \quad , \tag{3}$$

$$\tau = 0.5(S_V - S_H)\sin 2\theta \quad , \tag{4}$$

where σ_n and τ are the normal and shear stresses acting on a fault making an angle θ with the horizontal; S_V and S_H are the formation overburden and horizontal stresses; C is the cohesion strength and μ_f is the coefficient of internal friction. It is important to monitor changes in the reservoir pressure and stresses to reduce chances of CO_2 leakage through cap rock fracture or re-activation of any pre-existing fault.

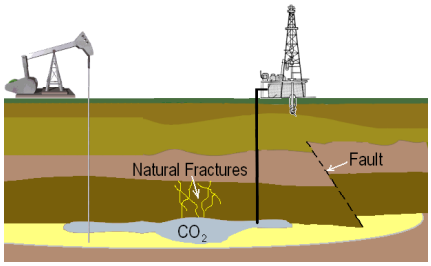

Figure 1: Schematic diagram of CO_2 (and water) injection to enhance production in a tertiary recovery project. Reservoir stresses need to be monitored to avoid CO_2 leakage through cap rock fracture or activation of any pre-existing fault.

This paper describes a new technique for the estimation of reservoir stresses at various stages of depletion or fluid injection using time-lapse analysis of borehole sonic data in a cased hole.

II. THEORY

Consider a borehole parallel to the X_3-axis and its cross-sectional plane parallel to the X_1-X_2- plane as shown in Figure 2.

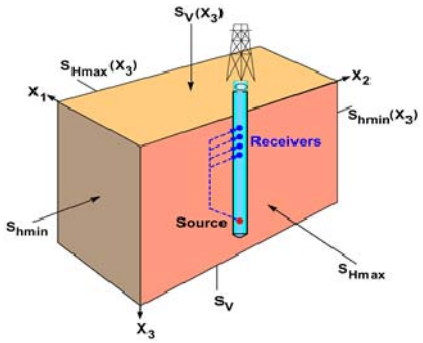

Figure 2: Schematic of a borehole in the presence of formation principal stresses with the borehole axis parallel to the overburden stress Sv and the maximum and minimum horizontal stresses S_{Hmax} and S_{hmin}, parallel to the X_1- and X_2-axis, respectively.

The overburden stress S_V is parallel to the X_3-axis, and the horizontal stress S_{Hmax} is in the X_1-X_3 plane. Processing of dipole data acquired by a transmitter aligned with the X_1-axis yields the shear modulus C_{55}, whereas the other orthogonal transmitter aligned with the X_2-axis yields the shear modulus C_{44}. The Stoneley data is used to obtain the shear modulus C_{66} in the borehole cross-sectional (X_1-X_2) plane. Sonic velocities and corresponding elastic moduli are functions of effective stresses in the propagating medium [1]-[4]. Figure 2 shows schematic of a borehole in a triaxially stressed formation where the effective stresses are defined in terms of the total formation stress and reservoir (or pore) pressure together with the Biot coefficient α.

The acoustoelastic theory relates changes in the effective shear moduli to incremental changes in the biasing stresses and strains from a reference state of the material [1]-[4]. Referred to an isotropically loaded reference state, formation shear moduli in the three orthogonal planes are the same (C_{44} =C_{55}=C_{66}=μ). When this rock is subject to anisotropic incremental stresses, changes in the three shear moduli are different and can be expressed as [3]

$$\Delta C_{55} = [C_{55} - \nu\, C_{144} + (1-\nu) C_{155}] \frac{\Delta\sigma_{11}}{2\mu\,(1+\nu)} \quad (7)$$
$$+ [C_{144} - (1+2\nu) C_{55} - 2\nu\, C_{155}] \frac{\Delta\sigma_{22}}{2\mu\,(1+\nu)}$$
$$+ [2\mu\,(1+\nu) + C_{55} - \nu\, C_{144} + (1-\nu) C_{155}] \frac{\Delta\sigma_{33}}{2\mu\,(1+\nu)} \quad ,$$

where ΔC_{55} is obtained from the fast-dipole shear slowness and formation bulk density, C_{55}(=μ) is the shear modulus, Y [=2μ(1+ν)], and ν are the Young's modulus, and Poisson's ratio, respectively; C_{144} and C_{155} are nonlinear constants referred to the chosen reference state; and $\Delta\sigma_{33}$, $\Delta\sigma_{11}$, and $\Delta\sigma_{22}$, respectively, denote changes in the *effective* overburden, maximum horizontal, and minimum horizontal stresses from an effectively isotropic reference state. Similarly, changes in the other two moduli ΔC_{44} and ΔC_{66} can be expressed described by the following two equations

$$\Delta C_{44} = [-(1+2\nu) C_{44} + C_{144} - 2\nu\, C_{155}] \frac{\Delta\sigma_{11}}{2\mu\,(1+\nu)} \quad (8)$$
$$+ [-\nu\, C_{144} + C_{44} + (1-\nu) C_{155}] \frac{\Delta\sigma_{22}}{2\mu\,(1+\nu)}$$
$$+ [2\mu\,(1+\nu) + C_{44} - \nu\, C_{144} + (1-\nu) C_{155}] \frac{\Delta\sigma_{33}}{2\mu\,(1+\nu)} \quad ,$$

where ΔC_{44} is obtained from the slow-dipole shear slowness and formation bulk density at a given depth, and C_{44} (=μ) is the shear modulus in the chosen reference state.

$$\Delta C_{66} = [\mu(1+\nu) + C_{66} - \nu\, C_{144} + (1-\nu) C_{155}] \frac{(\Delta\sigma_{11} + \Delta\sigma_{22})}{2\mu\,(1+\nu)} \quad (9)$$
$$+ [-(1+2\nu) C_{66} + C_{144} - 2\nu C_{155}] \frac{\Delta\sigma_{33}}{2\mu\,(1+\nu)} \quad ,$$

where ΔC_{66} is obtained from the Stoneley shear slowness dispersion and formation bulk density at a given depth, and C_{66} (= μ) is the shear modulus in the chosen reference state.

III. DIFFERENCE EQUATIONS USING THE FAR-FIELD SHEAR MODULI

A reservoir sand in the absence of formation stresses and fluid mobility behaves like an isotropic material characterized by a shear and bulk moduli. However, a complex shaly-sand reservoir is characterized by anisotropic elastic stiffnesses. Anisotropic elastic stiffnesses and the three shear moduli are affected by (a) structural anisotropy; (b) stress-induced anisotropy; and (c) formation mobility. Structural anisotropy caused by clay microlayering in shales is described by transversely-isotropic (TI-) anisotropy characterized by the horizontal shear modulus C_{66} larger than the vertical shear moduli C_{44}=C_{55}, in the absence of any stress-induced effects. Shales are impermeable and do not constitute part of a conventional reservoir. Since the effect of formation stresses on the effective shear moduli in a sand and shale interval are substantially different, it is necessary to apply appropriate corrections to the measured shear moduli in the estimation of formation stress magnitudes in shale intervals.

The three shear moduli can be estimated from borehole sonic data. As described earlier, differences in the effective shear moduli are related to differences in the principal stress magnitudes through an acoustoelastic coefficient defined in terms of formation nonlinear constants referred to a chosen reference state and for a given formation lithology [2]-[4]. Next we assume that the X_1-, X_2-, and X_3-axes, respectively, are parallel to the maximum horizontal (σ_H), minimum horizontal (σ_h), and vertical (σ_V) stresses. Under these circumstances, equations (10) yield difference equations in the effective shear moduli in terms of differences in the principal stress magnitudes through an acoustoelastic coefficient defined in terms of formation nonlinear constants referred to a chosen reference state and for a given formation lithology. The following three equations relate changes in the shear

moduli to corresponding changes in the effective principal stresses [2]:

$$C_{44}-C_{66}=A_E(\sigma_{33}-\sigma_{11}) \quad , \tag{10a}$$

$$C_{55}-C_{66}=A_E(\sigma_{33}-\sigma_{22}) \quad , \tag{10b}$$

$$C_{55}-C_{44}=A_E(\sigma_{11}-\sigma_{22}) \quad , \tag{10c}$$

where $\sigma_{33}(=\sigma_V)$, $\sigma_{11}(=\sigma_H)$, and $\sigma_{22}(=\sigma_h)$ denote the effective overburden, maximum horizontal, and minimum horizontal stresses, respectively; and

$$A_E = 2+\frac{c_{456}}{\mu}, \tag{11a}$$

is the acoustoelastic coefficient, C_{55} and C_{44} denote the shear moduli for the fast and slow shear waves, respectively; $C_{456}=(C_{155}-C_{144})/2$, is a formation nonlinear parameter that defines the acoustoelastic coefficient; and μ represents the shear modulus in a chosen reference state. However, only two of the three difference equations in (10) are independent.

The presence of unbalanced stress in the cross-sectional plane of borehole causes dipole shear wave splitting and the observed shear slowness anisotropy can be used to calculate the acoustoelastic coefficient A_E from equation (10c) provided we have estimates of the two principal stresses (σ_{11} and σ_{22}) as a function of depth. Note that the dipole shear waves are largely unaffected by the fluid mobility. We can then estimate the stress-induced change in the Stoneley shear modulus C_{66} using equations (10a) and (10b), and the effective stress magnitudes σ_V, σ_H, and σ_h at a given depth.

When we have estimates of the minimum horizontal (σ_{22}) and overburden (σ_{33}) stress magnitudes as a function of depth, we can determine the acoustoelastic parameter A_E in terms of the far-field shear moduli C_{55} and C_{66} using the relation

$$A_E = \frac{c_{55}-c_{66}}{\sigma_V-\sigma_h}, \tag{11b}$$

where we assume that the effects of permeability on these shear moduli are essentially similar and any small difference can be neglected.

Once we have determined the acoustoelastic parameter for a given lithology interval, we can determine the maximum horizontal stress σ_H magnitude as a function of depth from the following equation

$$\sigma_H = \sigma_h + \frac{c_{55}-c_{44}}{A_E}, \tag{12a}$$

where C_{55} and C_{44} denote the fast and slow dipole shear moduli, respectively. Similarly, the minimum horizontal stress σ_h magnitude as a function of depth from the following equation

$$\sigma_h = \sigma_V - \frac{c_{55}-c_{66}}{A_E}, \tag{12b}$$

Hence, we can estimate formation horizontal stress magnitudes as a function of depth in terms of the three shear moduli C_{44}, C_{55}, and C_{66}, and the acoustoelastic coefficient A_E.

IV. Reservoir Stresses After Depletion Or Injection

Consider a vertical fluid-filled borehole parallel to the X_3-direction, and the maximum and minimum horizontal stresses parallel to the X_1- and X_2-directions, respectively. Sonic data acquired in a fluid-filled open or cased hole can be inverted to obtain the three far-field formation shear moduli. These three shear moduli together with the effective overburden and minimum horizontal stresses in a baseline survey provide an estimate of the maximum horizontal stress magnitude together with an acoustoelastic coefficient as given by the following equations:

$$A_E = \frac{C_{55}^B - C_{66}^B}{\sigma_V^B - \sigma_h^B}, \tag{14}$$

$$\sigma_H^B = \sigma_h^B + \frac{(C_{55}^B - C_{44}^B)}{A_E}, \tag{15}$$

where the superscript "B" denotes quantity *before* depletion or injection, and the effective stress σ_{ij} is given by

$$\sigma_{ij} = S_{ij} - \alpha\,\delta_{ij}\,P_P \quad , \tag{16}$$

where S_{ij} is the total stress, δ_{ij} is the Kronecker delta, α is the Biot coefficient, and P_P is the pore or reservoir pressure. The total overburden stress is estimated by integrating the bulk density from the surface to the depth of interest and the minimum horizontal stress is estimated by a mini-frac or extended leak-off tests [5]-[6].

The difference between the effective overburden and minimum horizontal stress *after* depletion and injection can be described by

$$\sigma_V^A - \sigma_h^A = \frac{(C_{55}^A - C_{66}^A)}{A_E} \quad , \tag{17}$$

where the superscript "A" denotes quantity estimated *after* depletion or injection, and it is assumed that the overburden stress is essentially the same as before depletion or injection. When the depletion of the reservoir is rather extensive that there is no bridging effect, the total vertical stress will be carried by the formation and the total vertical stress will be essentially the same as before.

The total minimum and maximum horizontal stresses after depletion can then be given by the following equations

$$S_h^A = S_V^B - (\sigma_V^A - \sigma_h^A) \quad , \tag{18}$$

$$S_H^A = S_V^B - (\sigma_V^A - \sigma_H^A) \quad , \tag{19}$$

where S_h^A and S_H^A denote the total minimum and maximum horizontal stresses in the reservoir after depletion or injection.

V. An Illustrative Example

Processing of monopole and dipole waveforms recorded at an array of hydrophone receivers yields the lowest-order axi-symmetric Stoneley and borehole flexural dispersions as shown in Figures 3. Notice that the fast and slow flexural dispersions correspond to the dipole transmitter aligned parallel to the maximum σ_H and minimum σ_h horizontal stress directions, respectively. Figures 3a and 3b show the Stoneley, fast-dipole and slow-dipole dispersions at a first reference

depth after fluid injection over a period of about 14 months. Figures 3c and 3d display similar results at a second depth in the same reservoir acquired before and after *fluid injection*.

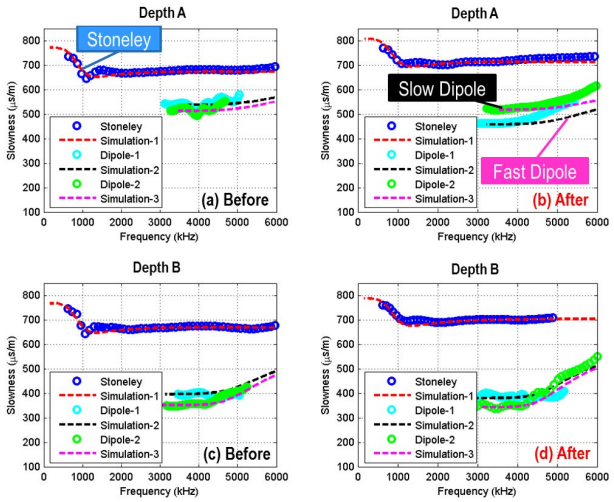

Figure 3: Comparison of measured and simulation results for the Stoneley, fast-, and slow-dipole dispersions acquired before and after *fluid injection* into a reservoir.

Inversion of the Stoneley dispersion from about 1.5 to 3 kHz yields the far-field shear modulus C_{66} [3]-[7]. In addition, low-frequency asymptotes of the fast- and slow-dipole dispersions directly provide estimates of the shear moduli C_{55} and C_{44} in the two borehole axial planes containing azimuths of the maximum and minimum horizontal stress directions, respectively. Figure 4 compares the three shear moduli before and after fluid injection at a reference depth A in a depleted reservoir at a select reference depth.

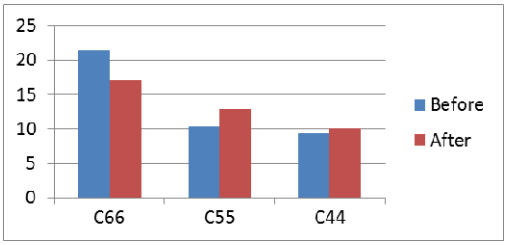

Figure 4: Corresponding changes in the shear moduli C66, C55, and C44 before and after fluid injection.

We assume that there is no bridging effect across the reservoir layer and the total vertical stress is essentially the same as before the fluid injection. Under these circumstances, an increase in the reservoir pressure would cause the horizontal stresses to increase as well. Figure 5 displays comparison of the maximum and minimum horizontal stresses caused by the fluid injection in a depleted reservoir whereas the overburden stress S_V is assumed to be the same before and after the fluid injection.

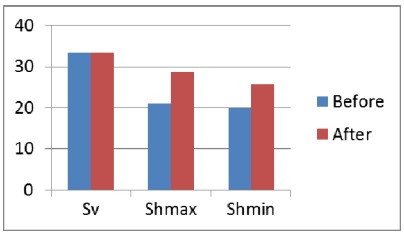

Figure 5: Estimated corresponding changes in the reservoir stresses before and after fluid injection.

V. Discussion And Conclusion

Time-lapse seismic surveys can detect acoustic impedance changes on the order of 3 to 9% in CO_2-saturated rocks that are good indicators of qualitative changes in the reservoir pressure and saturation. Sonic data in cased holes acquired before and after reservoir depletion or injection exhibits discernible changes on the order of 2 to 6% in the compressional velocity together with the borehole Stoneley and dipole flexural dispersions. Time-lapse sonic data acquired in a reservoir interval before and after production or fluid injection can provide estimates of changes in the reservoir stresses. Estimated maximum and minimum horizontal stresses after depletion or injection together with estimated reservoir pressure can then be used to calculate an injection pressure threshold to avoid fracture creation. They can also be used to determine a reservoir pressure window that will mitigate chances of shear slippage occurring along an existing fault. Therefore, it is necessary to monitor such changes in reservoir stresses as a function of changes in reservoir pressures to avoid reactivation of an existing fault or introduction of unwanted fractures in the cap-rock that would result in CO_2 leakage.

References

[1] A.N. Norris, B.K. Sinha, and S. Kostek, "Acoustoelasticity of solid/fluid composite systems", *Geophys. J. Internat.*, **118**, (1994) 439-446.

[2] B.K. Sinha, B. Vissapragada, L. Renlie and E. Skomedal, "Horizontal stress magnitude estimation using the three shear moduli – A Norwegian Sea Case study", SPE 103079, Annual Technical Conference and Exhibition, (2006).

[3] B.K. Sinha, B. Vissapragada, L. Renlie, and S. Tysse, "Radial Profiling of the Three Formation Shear Moduli and its Application to Well Completions", *Geophysics* (71), (2006) 65-77.

[4] B.K. Sinha, B. Vissapragada, A.S. Wendt, M. Kongslien, H. Eser, E. Skomedal, L. Renlie, and E.S. Pedersen, "Estimation of Formation Stresses Using Radial Variation of the Three Shear Moduli in a Well - A Case Study from a High-Pressure and High-Temperature Field in the Norwegian North Sea". *SPE* 109842 (2007).

[5] A.M. Raaen, P. Horsud, H. Kjorholt, and D. Okland, "Improved routine estimation of the minimum horizontal stress component from extended leak-off tests," International Journal of Rock Mechanics & Mining Sciences 43 (2006) 37-48.

[6] J. Desroches, and A. Kurkjian, "Applications of Wireline Stress Measurements", SPE 48960 (1998).

[7] J. Yang, B.K. Sinha, and T.M. Habashy, "Estimation of formation shear and borehole-fluid slownesses using sonic dispersion data in well-bonded cased boreholes", Geophysics, vol. 76(6), November-December 2011.